Angewandte Chemie
Eine Zeitschrift der Gesellschaft Deutscher Chemiker

Supporting Information

69451 Weinheim, Germany

Molecular Symmetry and Solution Phase Structure Interrogated by Hyper-Rayleigh Scattering Depolarization Measurements: Insights for Elaborating Highly Hyperpolarizable D_2-Symmetric Supermolecules

Timothy V. Duncan,† Kai Song,‡ Sheng-Ting Hung,‡ Ivan Miloradovic,† Animesh Nayak,† André Persoons,‡ Thierry Verbiest,‡ Michael J. Therien, †* and Koen Clays‡*

†Department of Chemistry, University of Pennsylvania, Philadelphia, Pennsylvania, USA.

‡Department of Chemistry, University of Leuven, Leuven, Belgium

* Corresponding authors

Experimental:

Materials. Inert atmosphere manipulations were carried out under nitrogen prepurified by passage through an O_2 scrubbing tower (Schweizerhall R3-11 catalyst) and a drying tower (Linde 3-Å molecular sieves). Air-sensitive solids were handled in a Braun 150-M glove box. Standard Schlenk techniques were employed to manipulate oxygen and moisture sensitive chemicals. Tetrahydrofuran (Fisher Scientific, HPLC grade) was distilled from potassium/benzophenone, while diethylamine and triethylamine were distilled from CaH_2; DMF (anhydrous), toluene (anhydrous), 1,2-dichloroethane (anhydrous), and *N*,*N*-diisopropylethylamine (redistilled, 99.5 %) were used as received from Aldrich. $Pd(PPh_3)_4$ and CuI were obtained from either Aldrich or Strem.. The syntheses of ruthenium(II) 5-[4-ethynyl-(2,2′;6′,2″-terpyridinyl)]-15-[4′-nitrophenyl)ethynyl]bis[10,20-bis(3,3-dimethyl-1-butyloxy)phenyl)porphinato]zinc(II)-bis(2,2′;6′2″-terpyridine)$^{2+}$ bis-hexafluorophosphate (**RuPZnA)**,[1] bisosmium(II) 5,15-bis[4′-ethynyl-(2,2′;6′,2″-terpyridinyl)]bis[10,20-bis(2′,6′-bis(3,3-dimethyl-1-butyloxy)phenyl)porphinato]zinc(II)-bis(2,2′;6′,2″)terpyridine)$^{4+}$ tetrakis-hexafluorophosphate (**OsPZnOs**),[2] bis[(5,5′,-10,20-di(2′,6′-bis(3,3-dimethylbutoxy)phenyl)porphinato)zinc(II)]ethyne (**PZnEPZn**) [3]and bis[(5,5′,-10,20-di(2′,6′-bis(3,3-dimethylbutoxy)phenyl)porphinato)zinc(II)]butadiyne (**PZnE$_2$PZn**)[3] have been reported elsewhere. Precursors [5,15-diethynyl-10,20-bis(heptafluoropropyl)-porphinato]zinc(II) (**R$_f$PZn**), [5-ethynyl-10,20-bis(2′,6′-bis(3,3-dimethyl-1-butyloxy)phenyl)-

porphinato)zinc(II) **(EPZn),** 4-bromo-2,2′:6′,2″-terpyridine (**brtpy**)[1] ruthenium(II) (4-bromo-2,2′:6′,2″-terpyridine)(2,2′:6′,2″-terpyridine) bis(hexafluorophosphate (**Ru(brtpy)(tpy)**)[1] and osmium (II) (4-bromo-2,2′:6′,2″-terpyridine)(2,2′:6′,2″-terpyridine bis(hexafluorophosphate (**Os(brtpy)(tpy)**)[1] were prepared according to established literature procedures. Starting materials ruthenium(II) bis(4-bromo-2,2′:6′,2″-terpyridine) bis(hexafluorophosphate (**Ru(brtpy)$_2$**) and osmium(II) bis(4-bromo-2,2′:6′,2″-terpyridine) bis(hexafluorophosphate (**Os(brtpy)$_2$**) were isolated as side-products during the syntheses of (**Ru(brtpy)(tpy)**) and (**Os(brtpy)(tpy)**), respectively, as discussed in Uyeda, *et al*;[1] characterization details are provided below. All other reagents were purchased from Aldrich, Strem, or GFS chemicals and used without further purification unless specified otherwise.

Chromatographic purification (silica gel 60, 230-400 mesh, EM Scientific; Bio-Beads S-X1, Bio-Rad Laboratories) of all newly synthesized compounds was accomplished on the bench top. Purity and identification of the four new compounds in this work were determined by NMR spectroscopy and/or elemental analysis, as well as MALDI-TOF, as follows. For all compounds, clean (no extraneous non-trace peaks) ^{1}H NMR and ^{13}C NMR spectra were obtained. As no non-trace peaks not attributable to nuclei found in the desired compounds were observed in any of the NMR spectra (see Figures S7-S16 for spectra corresponding to the aromatic regions for each compound) we were able to conclude that the samples studied by HRS were >97% pure in all cases. In the case of the compounds containing heptafluoropropyl porphyrinic side chains (**RfRuPZnRfRu** and **RfOsPZnRfOs**), there was not a 1:1 correlation between the number of observed ^{13}C NMR spectral peaks and the number of carbon nuclei in the respective molecules due to known ^{13}C-^{19}F spin-spin coupling contributions; making peak assignments for these spectra would thus be difficult without sophisticated 2D experiments, the utilization of model compounds, or fluorine-decoupled 13C NMR spectra. As a result the purity and identity of these two compounds was thus further verified by ^{19}F NMR spectroscopy, which exhibited the correct number of ^{19}F peaks. The clean ^{19}F spectra are important to assess purity because they rule out the presence of other [(heptafluoropropyl)-porphinato]zinc(II) contaminants (e.g., residual starting materials, incomplete coupling products, etc.), which would also be the most likely

contaminants to give rise to a false HRS signal. Furthermore, for these two compounds, elemental analysis results were obtained that demonstrate acceptable purity. In the case of compounds **PZnRuPZn** and **PZnOsPZn**, the alkoxyphenyl porphyrinic side chains efficiently trap solvent molecules, which preclude the attainment of clean elemental analysis. However, the lack of fluorine nuclei in these compounds gave rise to a clear 1:1 correlation between the number of observed ^{13}C NMR spectral peaks and the number of carbon nuclei in the respective molecules, which again demonstrates proof of purity. Accurate MALDI-TOF data was also obtained on all compounds, demonstrating proof of identification.

Instrumentation. Electronic spectra were recorded on an OLIS UV/vis/near-IR spectrophotometry system that is based on the optics of a Cary 14 spectrophotometer.

^{1}H NMR and proton-decoupled ^{13}C NMR spectra were recorded on a 500 MHz AMX Bruker spectrometer (^{1}H NMR data acquired at 500.13 MHz and ^{13}C NMR data acquired at 125.76 MHz); ^{19}F NMR spectra of **RuR$_f$PZnRu** and **OsR$_f$PZnOs** were acquired on a 300 MHz Bruker spectrometer (^{19}F NMR data acquired at 282.23 MHz). All chemical shifts for ^{1}H NMR spectra are relative to that of TMS. All *J* values are reported in Hertz. The number of attached protons is found in parentheses following the chemical shift value. For ^{13}C NMR spectra, peaks are relative to the solvent (CD_3CN) ^{13}C resonance (~118.7 ppm). For ^{19}F NMR spectra, peaks are relative to that of $CFCl_3$.

MALDI-TOF mass spectroscopic data were obtained with either an Applied Biosystems Perceptive Voyager-DE instrument in the Laboratories of Dr. Virgil Percec (Department of Chemistry, University of Pennsylvania) or a PerSpective BioSystems Voyager-DE instrument in the Laboratories of Dr. William DeGrado (Department of Biochemistry and Biophysics, University of Pennsylvania School of Medicine). Samples were prepared as micromolar solutions in THF, and either dithranol (Aldrich) or α-cyano-4-hydroxy cinnamic acid (α-CHCA) was utilized as the matrix. Electrospray ionization (ESI-MS) and chemical ionization (CI-MS) data were obtained in the University of Pennsylvania Chemistry Mass Spectrometry Facility. Elemental analysis data was acquired by Robertson Microlit Laboratories (www.robertsonmicrolit.com).

Hyper Rayleigh Light Scattering (HRS) Measurements. The experimental values for the second-order nonlinear polarizability (first hyperpolarizability) and depolarization ratio have been determined by hyper-Rayleigh scattering experiments performed at λ_{inc} = 800 nm.[4] To ensure that the observed HRS signal at the second-harmonic wavelength is purely second-order scattering, and not due to multiphoton fluorescence, frequency-resolved femtosecond HRS experiments were performed. These measurements show neither a demodulation nor an increase in phase delay with increasing amplitude modulation, indicating the absence of any multiphoton fluorescence contribution to the observed HRS signals (Figure S4). This finding is in line with the results reported earlier for other members of the same class of (polypyridyl)ruthenium-(porphinato)zinc(II) chromophores.[1] The measurement of the first hyperpolarizability is a relative measurement, with the reference value at 800 nm being 340 x 10^{-30} esu for the $\beta_{yyy} = -\beta_{yxx} = -\beta_{xyx} = -\beta_{xxy}$ tensor components of the D_{3h} octopolar crystal violet molecule in methanol (the *z*-axis being the unique microscopic molecular axis).[5] The symmetry of the molecular scatterer is important, as it determines the number and the nature of the non-zero hyperpolarizability tensor components that contribute to the signal.[6] The depolarization ratio ρ is determined as the intensity ratio $\rho = I_{\parallel}/I_{\perp} = \langle\beta_{ZZZ}^2\rangle / \langle\beta_{YZZ}^2\rangle$ between the HRS signal intensity (I) for parallel ($I_{\parallel}$) and perpendicular ($I_{\perp}$) polarization between incoming fundamental (vertically polarized along the macroscopic laboratory *Z*-axis) and detected harmonic signal (polarized either along the same *Z*-axis for parallel and along the *Y*-axis for perpendicular polarization).[7-10] To accurately determine this ratio, the analyzing polarizer in front of the detector is rotated and the total HRS signal intensity is recorded as a function of angle between the two polarization states. From a fitting to this periodic pattern, an accurate depolarization ratio can be determined.

From the value of this ratio, an assumption about the approximate symmetry should be made to determine the appropriate hyperpolarizability tensor components from which to analyse the HRS intensity. High values for ρ suggest major dipolar contributions to the HRS response and a single major β_{zzz} component. Low values for ρ have been observed and predicted only for octopolar molecular symmetries. In D_{3h} symmetry, for example, 4

(identical) non-zero tensor components are analyzed (*e.g.*, crystal violet, *vide supra*). T_d symmetry, in contrast, 6 (identical) non-zero β_{ijk} components (i, j, k = x, y, z in Einstein notation convention) are relevant. D_{2d} symmetry, however, allows for the same non-zero β_{ijk} components as D_{3h} (based on the following symmetry elements: a C_2 axis (*z*), 2 mirror planes, and a S_4 screw axis), and thus also defines an octopolar molecular symmetry. For the lower D_2 symmetry, three sets of two identical hyperpolarizability tensor components ($\beta_{xyz} = \beta_{xzy}$, $\beta_{yxz} = \beta_{yzx}$, $\beta_{zxy} = \beta_{zyx}$) exist, based on the symmetry for second-harmonic generation ($\beta_{ijk} = \beta_{ikj}$, i, j, k = x, y, z). Note that the difference between, *e.g.*, β_{xyz} and β_{yxz}, then should give rise to a quadrupolar response. This quadrupolar response, however, can be taken as small, if not negligible.[11] Note that in the limit of Kleinman symmetry, the magnitude of the quadrupolar response is strictly zero. Therefore, all molecules under study having a depolarization ratio (ρ) ≤ 1.9 have been analysed assuming 6 identical and nonzero β_{ijk} components (i, j, k = x, y, z) components, while the molecules with ρ ≥ 2.9 have been analysed in the context of a single major β_{zzz} component.

Synthesis of MR_fPZnM (M = Ru,Os):

Osmium(II)[5-(4'-ethynyl-(2,2';6'2''-terpyridinyl))osmium(II)-15-(4'-ethynyl-(2,2';6'2''-terpyridinyl))-10,20-bis(heptafluoropropyl)-porphinato]zinc(II)-bis(2:2';6':2''-terpyridine)$^{4+}$ tetrakis-hexafluorophosphate [OsR_fPZnOs]. **R_fPZn** (40 mg, 0.053 mmol, 1 eqv), **Os(brtpy)(tpy)** (135 mg, 0.132 mmol, 2.5 eqv.), triethylamine (3 mL), and CH_3CN (60 mL) were placed in a 100-mL Schlenk tube. The solution was degassed via three freeze-pump-thaw cycles, following which $Pd_2(dba)_3$ (~15 mg, 0.016 mmol, 0.3 eqv) and $AsPh_3$ (44 mg, 0.143 mmol, 2.7 eqv.) were added via cannula. The reaction mixture was stirred under N_2 at 60 °C for 3 h, the solution was cooled to room temperature, and the solvent was removed. The product was purified by silica column chromatography using 90:9:1 CH_3CN:H_2O:saturated $KNO_{3(aq)}$ as the eluant. **$OsP_{Rf}ZnOs$** was eluted as a dark brown band; volume of the product fraction was reduced to 20 mL and ammonium hexafluorophosphate (1.5 g) in 20 ml of water was added, producing a brown-green precipitate. The product was filtered, washed successively with water and ether, and dried to give the final product as the hexafluorophosphate salt (Yield = 140 mg, 91% based on **R_fPZn** starting material). ^{1}H NMR

(500 MHz, CD_3CN): 10.28 (d, 4H, *J* = 4.7 Hz), 9.77 (br m, 4H), 9.46 (s, 4H), 8.84 (d, 4H, *J* = 8.3 Hz), 8.83 (ddd, 4H, *J* = 8.3 Hz, *J′* = 1.3 Hz, *J″* = 0.8 Hz), 8.53 (ddd, 4H, *J* = 8.2 Hz, *J′* = 1.3 Hz, *J″* = 0.8 Hz), 8.03 (t, 2H, *J* = 8.3 Hz), 7.96 (ddd, 4H, *J* = 7.8 Hz, *J′* = 7.5 Hz, *J″* = 1.4 Hz), 7.84 (ddd, 4H, J = 7.9 Hz, *J′* = 7.5 Hz, *J″* = 1.5 Hz), 7.53 (ddd, 4H, *J* = 5.9 Hz, *J′* = 1.5 Hz, *J″* = 0.8 Hz), 7.36 (ddd, 4H, J = 5.7 Hz, *J′* = 1.4 Hz, J″ = 0.8 Hz), 7.23 (ddd, 4H, *J* = 6.6 Hz, *J′* = 5.7 Hz, *J″* = 1.3 Hz), 7.18 (ddd, 4H, *J* = 6.7 Hz, *J′* = 6.0 Hz, *J″* = 1.3 Hz). ^{13}C NMR (500 MHz, CD_3CN): δ 161.088, 161.030, 156.535, 156.163, 154.176, 154.110,.154.048, 153.772, 150.592, 139.527(br), 137.062, 135.087(br), 134.568, 130.462, 129.963, 129.355, 129.146, 126.310, 126.189, 126.081, 125.720, 124.090, 108.717, 108.090, 107.915, 107.753, 102.920, 100.842, 95.045. ^{19}F NMR (300 MHz, CD_3CN): δ -71.62 (d, *J* = 705.5 Hz, PF_6^-), -76.86 (m), -78.52 (t, *J* = 12 Hz), -118.10 (m). MS (MALDI-TOF): *m*/*z*: 2358.14 $(M-2PF_6)^+$ (calcd for $C_{90}H_{50}F_{26}N_{16}P_2Os_2Zn$: 2357.22); *m*/*z*: 2212.31 $(M-3PF_6)^+$ (calcd for $C_{90}H_{50}F_{20}N_{16}POs_2Zn$: 2212.26); *m*/*z*: 2067.24 $(M-4PF_6)^+$ (calcd for $C_{90}H_{50}F_{14}N_{16}Os_2Zn$: 2067.29). Elemental analysis: C = 40.13%, H = 1.61%, N = 8.24% (calcd: C = 40.83%, H = 1.90%, N = 8.47%).

Ruthenium(II)[5-(4'-ethynyl-(2,2';6'2''-terpyridinyl))ruthenium(II)-15-(4'-ethynyl-(2,2';6'2''-terpyridinyl))-10,20-bis(heptafluoropropyl)-porphinato]zinc(II)-bis(2:2';6':2''-terpyridine)$^{4+}$ tetrakis-hexafluorophosphate [RuR_fPZnRu]. **R_fPZn** (40 mg, 0.053 mmol, 1 eqv), **Ru(brtpy)(tpy)** (124 mg, 0.132 mmol, 2.5 eqv), triethylamine (3 mL), and CH_3CN (60 mL) were placed in a 100-mL Schlenk tube. The solution was degassed via three freeze-pump-thaw cycles, following which $Pd_2(dba)_3$ (~15 mg, 0.016 mmol, 0.3 eqv) and $AsPh_3$ (44 mg, 0.143 mmol, 2.7 eqv), were added via cannula. The reaction mixture was stirred under N_2 at 60 °C for 3 h, the solution was cooled to room temperature, and the solvent was removed. The product was purified by silica column chromatography using 90:9:1 CH_3CN:H_2O:saturated $KNO_{3(aq)}$ as the eluant. **RuR_fPZnRu** was eluted as a dark brown band; volume of the product fraction was reduced to 20 mL and ammonium hexafluorophosphate (1.5 g) in 20 ml of water was added, producing a brown-green precipitate. The product was filtered, washed successively with water and ether, and dried to give the final product as the hexafluorophosphate salt (Yield = 130 mg, 89% based on **R_fPZn** starting material). ^1H NMR (500 MHz, CD_3CN): 10.29 (d, 4H, *J* = 4.9 Hz), 9.78 (br m,

4H), 9.47 (s, 4H), 8.84 (d, 4H, *J* = 7.8 Hz) 8.82 (d, 4H, *J* = 8.2 Hz), 8.55 (d, 4H, *J* = 8.1 Hz), 8.49 (t, 2H, *J* = 8.3 Hz), 8.10 (t, 4H, *J* = 7.8 Hz), 7.98 (t, 4H, *J* = 7.8 Hz), 7.56 (d, 4H, *J* = 5.6 Hz), 7.46 (d, 4H, J = 5.5 Hz), 7.29 (t, 4H, *J* = 6.5 Hz) 7.25 (t, 4H, *J* = 6.5 Hz). ^{13}C NMR (500 MHz, CD_3CN): δ 159.414, 159.244, 157.162, 156.624, 154.039(br), 153.698, 154.039(br), 153.698, 150.751, 139.697, 137.729, 137.614, 135.194(br), 134.642, 131.393, 129.229, 128.953, 126.809, 126.014, 125.946, 125.275,108.245, 108.077, 107.888. ^{19}F NMR (300 MHz, CD_3CN): δ-71.62 (d, *J* = 705.5 Hz, PF_6^-),, -76.98 (m), -78.54 (t, *J* = 12 Hz), -118.17 (m). MS (MALDI-TOF): *m*/*z*: 2179.97 $(M\text{-}2PF_6)^+$ (calcd for $C_{90}H_{50}F_{26}N_{16}P_2Ru_2Zn$: 2178.90); *m*/*z*: 2034.66 $(M\text{-}3PF_6)^+$ (calcd for $C_{90}H_{50}F_{20}N_{16}PRu_2Zn$: 2033.94); *m*/*z*: 1891.44 $(M\text{-}4PF_6)^+$ (calcd for $C_{90}H_{50}F_{14}N_{16}Ru_2Zn$: 1888.97). Elemental analysis: C = 43.56%, H = 2.19%, N = 8.13% (calcd: C = 43.78%, H = 2.04%, N = 9.08%).

Synthesis of PZnMPZn (M = Ru,Os):

Ruthenium(II) bis(4-bromo-2,2′:6′,2″-terpyridine) bis(hexafluorophosphate (Ru(brtpy)$_2$). This species was isolated as a side product during the synthesis of **Ru(brtpy)(tpy)**; see reference 1. ^{1}H NMR (500 MHZ, CD_3CN): δ 8.99 (s, 4H), 8.51 (dd, 4H, *J* = 8.0 Hz, *J* = 0.8 Hz), 7.95 (td, 4H, *J* = 7.9 Hz, *J* = 1.5 Hz), 7.40 (d, 4H, *J* = 5.6Hz), 7.21 (ddd, 4H, *J* = 7.6 Hz, *J* = 5.7 Hz, *J* = 1.3 Hz)

Osmium(II) bis(4-bromo-2,2′:6′,2″-terpyridine) bis(hexafluorophosphate (Os(brtpy)$_2$). This species was isolated as a side product during the synthesis of **Os(brtpy)(tpy)**; see reference 1. ^{1}H NMR (500 MHZ, CD_3CN): δ 8.99 (s, 4H), 8.46 (d, 4H, *J* = 8.1 Hz), 7.82 (td, 4H, *J* = 7.9 Hz, *J* = 1.4 Hz), 7.26 (d, 4H, *J* = 5.9 Hz), 7.12 (ddd, 4H, *J* = 7.4 Hz, *J* = 5.9 Hz, *J* = 1.3 Hz)

Ruthenium(II) bis[5-(4′-ethynyl-(2,2′;6′,2″-terpyridinyl))-10,20-bis(2,6-bis(3,3-dimethyl-1-butyloxy)phenyl)porphinato)zinc(II)] bis(hexafluorophosphate) (PZnRuPZn). 1 equivalent of **Ru(brtpy)$_2$** (25 mg, 0.024 mmol) and 2.1 equivalents of **EPZn** (~50 mg, 0.052 mmol) were placed in an appropriately sized Schlenk flask equipped with a stirbar. 0.25 equivalents $Pd_2(dba)_3$ (5.6 mg, 0.0062 mmol) and 2.5 equivalents $AsPh_3$ (19 mg, 0.062 mmol) were added under nitrogen atmosphere. A solvent mixture consisting of freshly-opened HPLC grade 6:3:1 MeCN:THF:triethylamine was degassed by a stream of dry nitrogen for approximately 30 minutes. An appropriate volume (~50 mL) of this solvent mixture was

added to the reaction vessel via cannula, and the resulting mixture was heated on an oil bath at 55 °C overnight (approximately 14 h), or until the starting materials were consumed as shown by thin layer chromatography (90:9:1 MeCN:water:saturated aqueous KNO_3 as eluent). The reaction mixture was then cooled to room temperature and concentrated to dryness by rotary evaporation. The crude product was purified by column chromatography using 90:9:1 MeCN:water:saturated aqueous KNO_3 as eluent; the product eluted generally second, following a small quantity of fast-moving homocoupled butadiyne-bridged porphyrin side-product, as a dark brown band. The desired fractions were combined and concentrated, but not to dryness. Excess ammonium hexafluorophosphate was added, followed by enough water to cause the precipitation of a dark brown-green solid, which was isolated by filtration, and washed successively with water and diethyl ether to yield the desired product. Additional column chromatography was performed if the level of purity was unsatisfactory by NMR spectroscopy. (Yield = 45 mg, 66% based on **Ru(brtpy)$_2$** starting material) ^{1}H NMR (500 MHZ, CD_3CN): δ 10.18 (s, 2H), 10.04 (d, 4H, *J* = 4.6 Hz), 9.43 (s, 4H), 9.31 (d, 4H, *J* = 4.3 Hz), 9.04 (d, 4H, *J* = 4.6 Hz), 8.85 (m, 8H), 8.10 (td, 4H, *J* =7.7 Hz, *J* = 1.4 Hz), 7.84 (t, 4H, *J* = 8.6 Hz), 7.66 (d, 4H, *J* = 6.1 Hz), 7.33 (td, 4H, *J* = 6.4 Hz, *J* = 1.2 Hz), 7.20 (d, 8H, *J* = 8.6 Hz), 4.03 (t, 16H, *J* = 7.1 Hz), 0.82 (t, 16H, *J* = 7.1 Hz) 0.20 (s, 72H). ^{13}C NMR (500 MHZ, CD_3CN): δ 161.449, 159.385, 156.825, 151.102, 153.094, 152.937, 151.582, 150.589, 139.677, 134.076, 133.530, 133.051, 132.909, 131.737, 131.110, 129.121, 126.236, 126.122, 121.962, 116.711, 109.553, 106.899, 104.497, 95.687, 94.251, 67.519, 43.057, 30.017, 29.695. MALDI-TOF: *m/z* 2461.98 (calculated for $C_{146}H_{154}N_{14}O_8RuZn_2$ $(M\text{-}2PF_6)^+$ 2462.44); *m/z* 2607.47 (calculated for $C_{146}H_{154}F_6N_{14}O_8PRuZn_2$ $(M\text{-}PF_6)^+$ 2607.40).

Osmium(II) bis[5-(4′-ethynyl-(2,2′;6′,2″-terpyridinyl))-10,20-bis(2,6-bis(3,3-dimethyl-1-butyloxy)phenyl)porphinato)zinc(II)] bis(hexafluorophosphate) (PZnOsPZn). 1 equivalent of **Os(brtpy)$_2$** (25 mg, 0.023 mmol) and 2.1 equivalents of **EPZn** (~45 mg, 0.0475 mmol) were placed in an appropriately sized Schlenk flask equipped with a stirbar. 0.25 equivalents $Pd_2(dba)_3$ (5.2 mg, 0.0057 mmol) and 2.5 equivalents $AsPh_3$ (17 mg, 0.057 mmol) were added under nitrogen atmosphere. A solvent mixture consisting of freshly-opened HPLC grade 6:3:1 MeCN:THF:triethylamine was degassed by a stream of dry nitrogen for

approximately 30 minutes. An appropriate volume (~50 mL) of this solvent mixture was added to the reaction vessel via cannula, and the resulting mixture was heated on an oil bath at 55 °C overnight (approximately 14 h), or until the starting materials were consumed as shown by thin layer chromatography (90:9:1 MeCN:water:saturated aqueous KNO_3 as eluent). The reaction mixture was then cooled to room temperature and concentrated to dryness by rotary evaporation. The crude product was purified by column chromatography using 90:9:1 MeCN:water:saturated aqueous KNO_3 as eluent; the product eluted generally second, following a small quantity of fast-moving homocoupled butadiyne-bridged porphyrin side-product, as a dark brown band. The desired fractions were combined and concentrated, but not to dryness. Excess ammonium hexafluorophosphate was added, followed by enough water to cause the precipitation of a dark brown-green solid, which was isolated by filtration, and washed successively with water and diethyl ether to yield the desired product. Additional column chromatography was performed if the level of purity was unsatisfactory by NMR spectroscopy. (Yield = 50 mg, 77% based on **Os(brtpy)$_2$** starting material) ^{1}H NMR (500 MHZ, CD_3CN): □ 10.14 (s, 2H), 10.00 (d, 4H, *J* = 4.6 Hz), 9.45 (s, 4H), 9.30 (d, 4H, *J* = 4.4 Hz), 9.03 (d, 4H, *J* = 4.5 Hz), 8.85 (d, 4H, *J* = 4.4 Hz); 8.82 (d, 4H, *J* = 8.3 Hz), 7.95 (td, 4H, *J* = 7.9 Hz, *J* = 1.4 Hz), 7.84 (t, 4H, *J* = 8.6 Hz), 7.53 (d, 4H, *J* = 5.3 Hz), 7.26 (td, 4H, *J* = 7.2 Hz, *J* = 1.3 Hz), 7.20 (d, 8H, *J* = 8.6 Hz), 4.01 (t, 16H, *J* = 7.1 Hz), 0.82 (t, 16H, *J* = 7.0 Hz) 0.20 (s, 72H). ^{13}C NMR (500 MHZ, CD_3CN): δ 161.483, 161.025, 156.380, 154..160, 153.192, 152.866, 151.532, 150.551, 139.479, 134.039, 133.517, 132.909, 132.033, 131.750, 131.069, 129.276, 126.229, 125.017, 121.967, 116.718, 109.535, 106.909, 104.625, 95.721, 93.072, 67.537, 43.033, 30.033, 29.717. MALDI-TOF: *m/z* 2551.41 (calculated for $C_{146}H_{154}N_{14}O_8OsZn_2$ $(M\text{-}2PF_6)^+$ 2551.54); *m/z* 2697.40 (calculated for $C_{146}H_{154}F_6N_{14}O_8OsPZn_2$ $(M\text{-}PF_6)^+$ 2696.24).

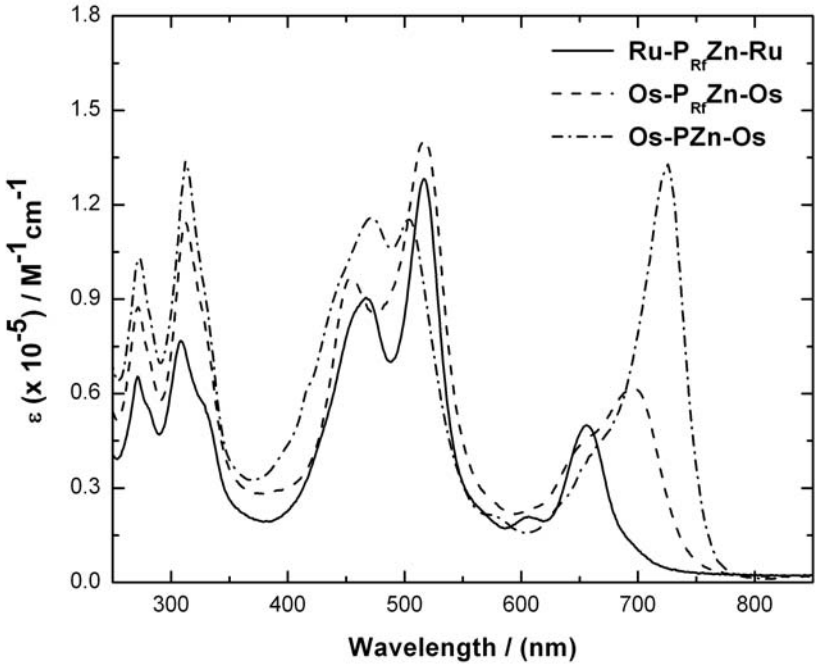

FIGURE S1. Comparative electronic absorption spectra of **OsR_fPZnOs**, **RuR_fPZnRu**, and **OsPZnOs**, acquired in acetonitrile.

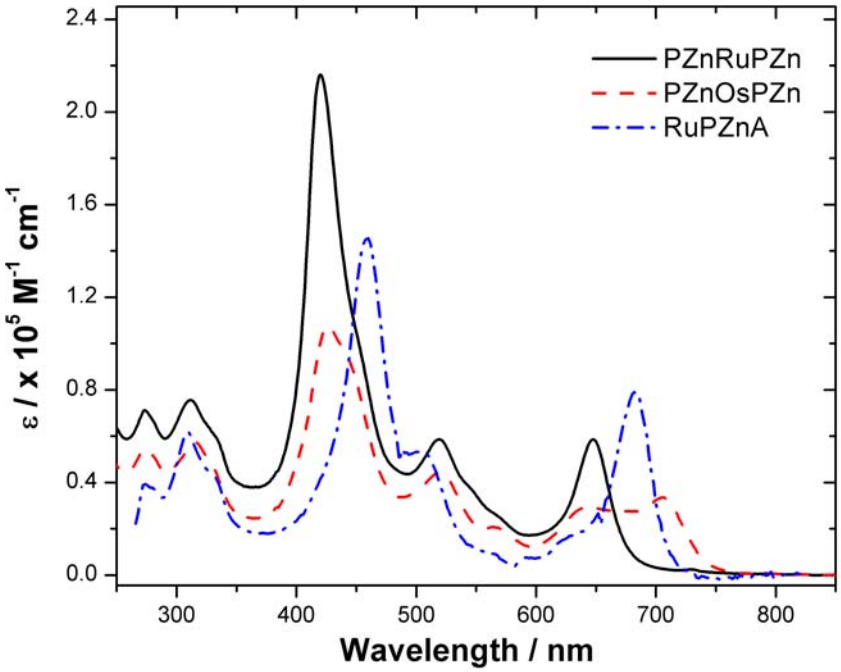

FIGURE S2. Comparative electronic absorption spectra of **PZnRuPZn**, **PZnOsPZn**, and **RuPZnA**, acquired in acetonitrile.

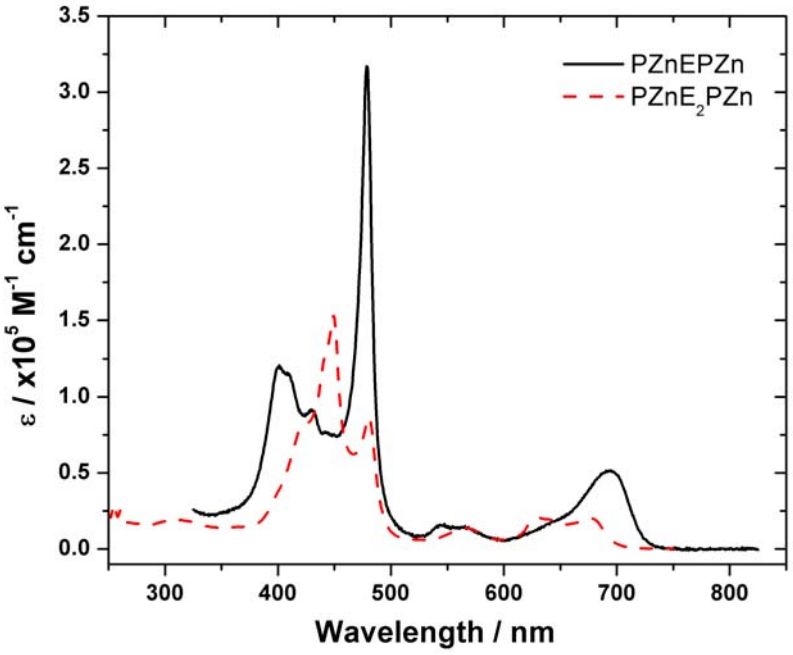

FIGURE S3. Comparative electronic absorption spectra of **PZnEPZn**, **PZnE$_2$PZn**, acquired in tetrahydrofuran.

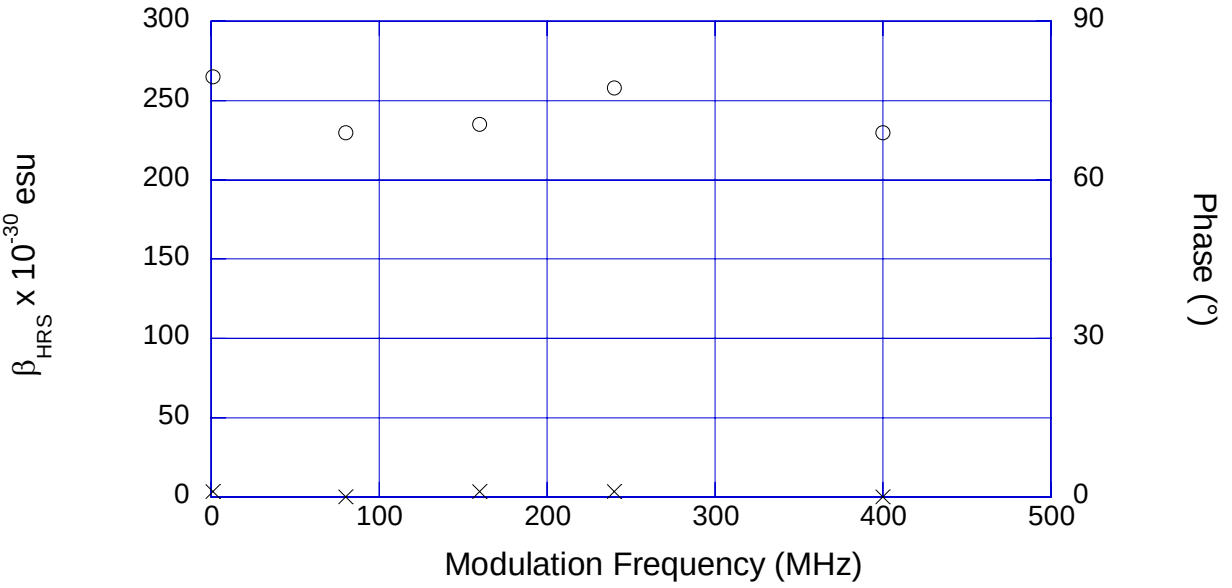

FIGURE S4. Experimentally determined β_{HRS} values ($\beta_{HRS}^2 = [<\beta_{ZZZ}^2> + <\beta_{YZZ}^2>] = 120/35\ \beta_{xyz}^2$ for octopolar (T_d, D_2 or D_{2d}) molecules) as a function of modulation frequency for **OsPZnOs**, showing the constant amplitude (○) and zero phase shift (×), to demonstrate the second-order scattering nature of the HRS signal.

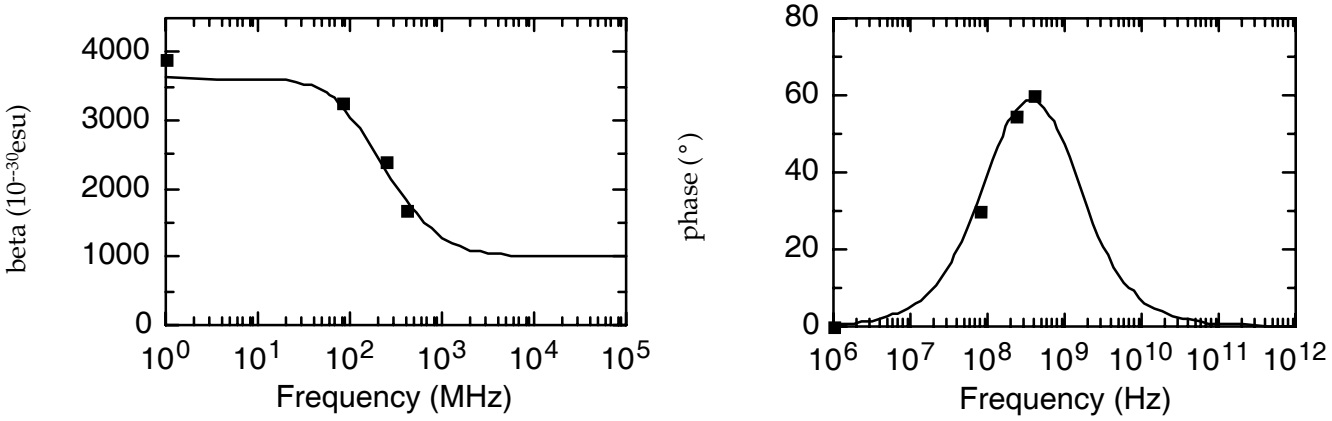

FIGURE S5. Demodulation of hyperpolarizability (left) and phase evolution (right) as a function of amplitude modulation frequency for compounds **PZnEPZn** as obtained from femtosecond hyper-Rayleigh scattering. The symbols represent the actual measured data (expressed as a β_{zzz}), the solid line results from the fitting to a single exponential fluorescence decay contributing to the scattering signal. The accurate fluorescence-free hyperpolarizability value is obtained as the high-frequency limit. Please note the difference with the frequency dependence shown in Fig. S4, where constant values for the hyperpolarizability and zero phases show the absence of fluorescence contributing to the signal.

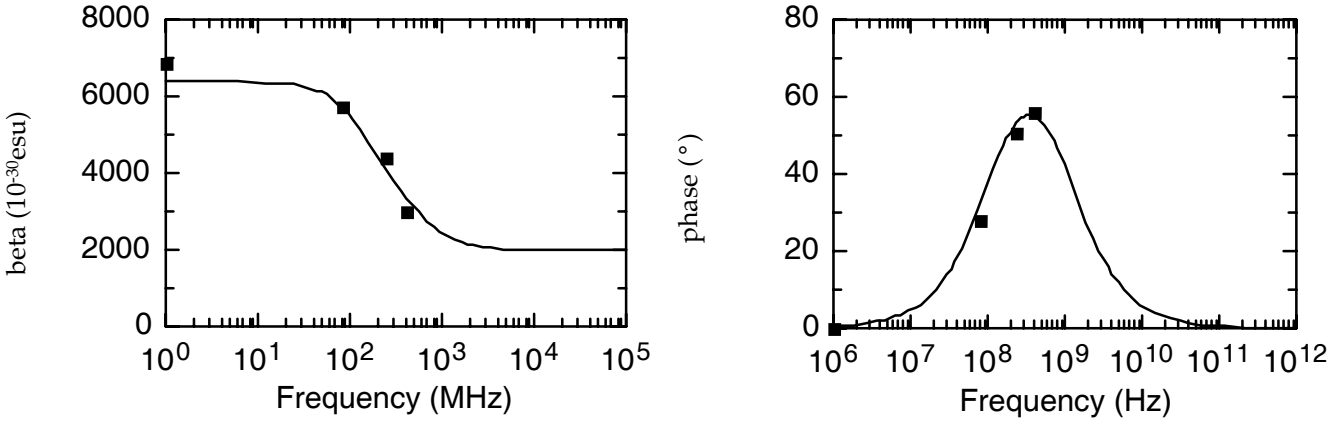

FIGURE S6. Demodulation of hyperpolarizability (left) and phase evolution (right) as a function of amplitude modulation frequency for compounds **PZnE2PZn** as obtained from femtosecond hyper-Rayleigh scattering. The symbols represent the actual measured data (expressed as a β_{zzz}), the solid line results from the fitting to a single exponential fluorescence decay contributing to the scattering signal. The accurate fluorescence-free hyperpolarizability value is obtained as the high-frequency limit. Please note the difference with the frequency dependence shown in Fig. S4, where constant values for the hyperpolarizability and zero phases show the absence of fluorescence contributing to the signal.

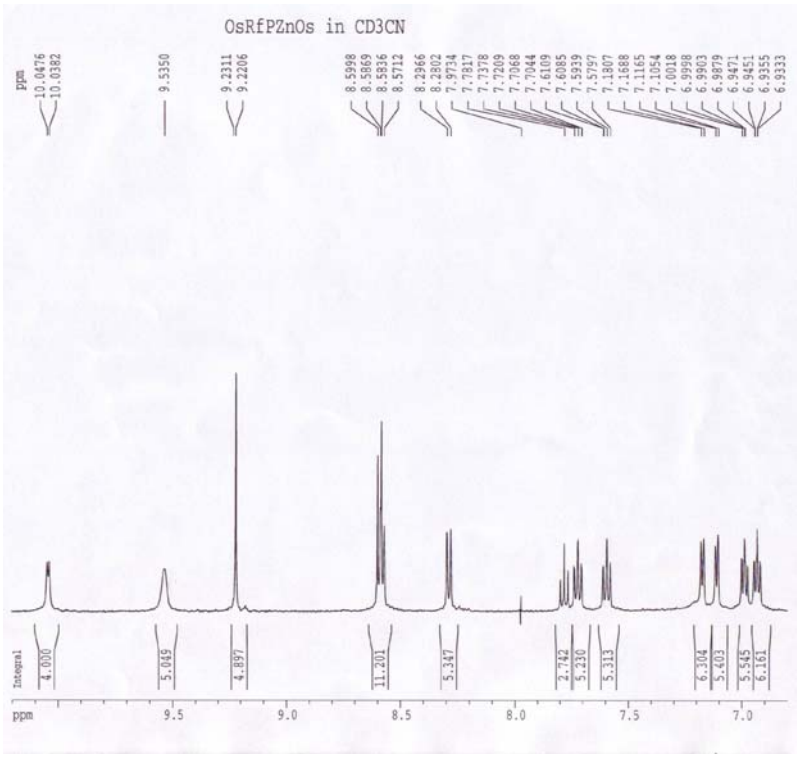

Figure S7A. Aromatic region of the ^{1}H NMR spectrum of **OsRfPZnOs** demonstrating identity and acceptable purity of the desired compound.

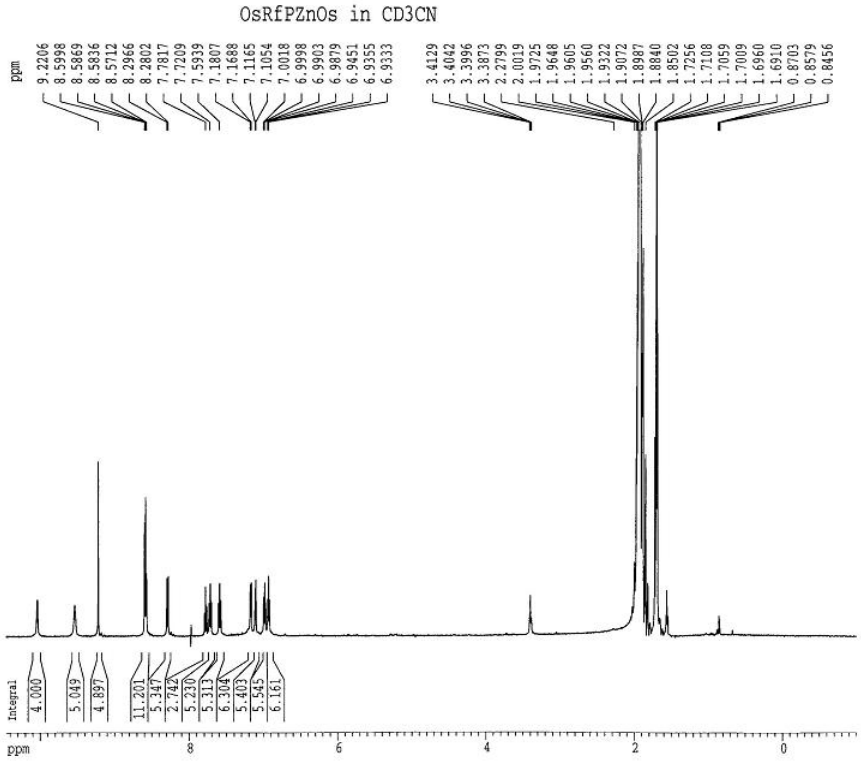

Figure S7B. Full ^{1}H NMR spectrum of **OsRfPZnOs**.

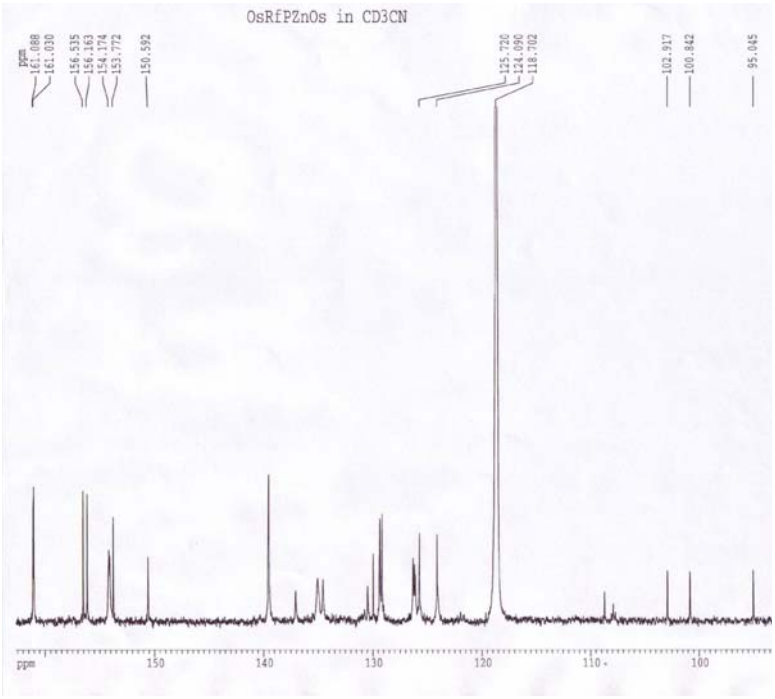

Figure S8A. Aromatic region of the proton-decoupled ^{13}C NMR spectrum of **OsRfPZnOs** demonstrating identity and acceptable purity of the desired compound. Note that the number of observed peaks does not exactly correspond to the number of carbon nuclei in this compound as a result of complications due to ^{13}C-^{19}F spin-spin interactions.

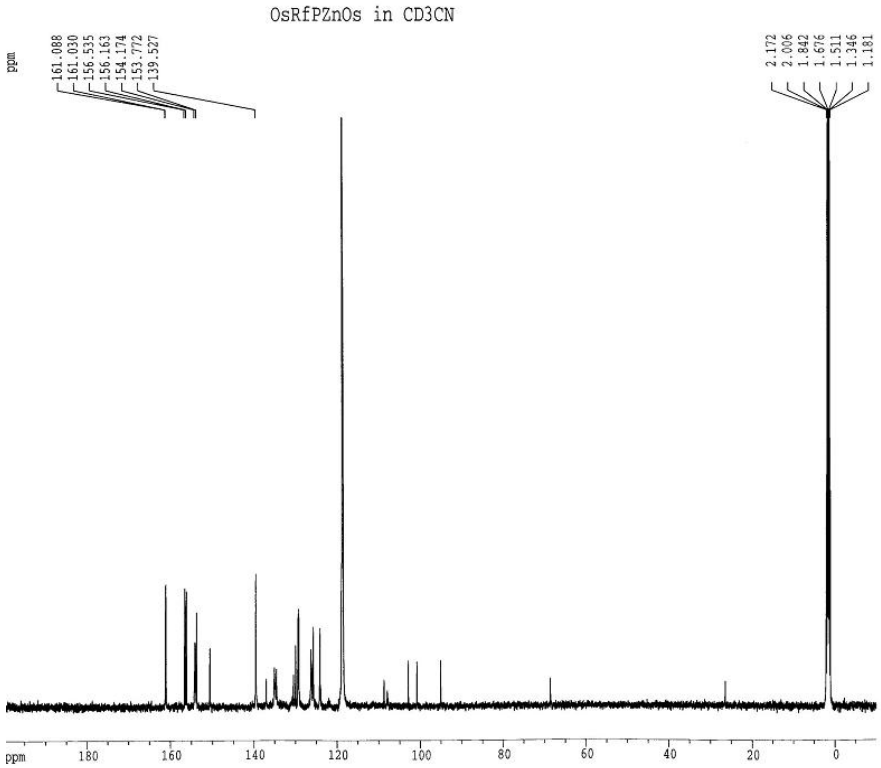

Figure S8B. Full proton-decoupled ^{13}C NMR spectrum of **OsRfPZnOs**.

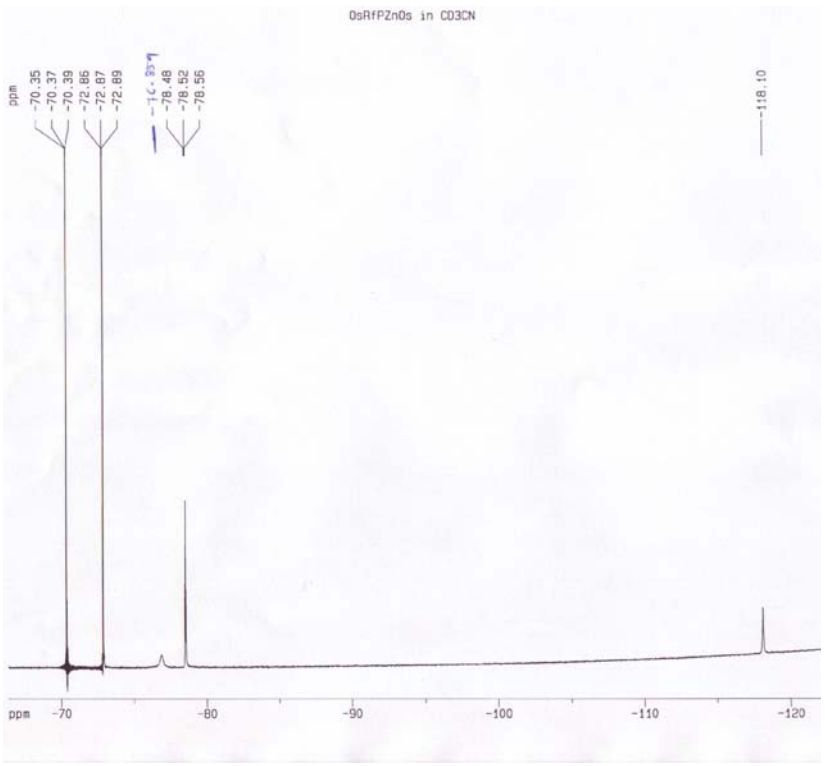

Figure S9. ^{19}F NMR spectrum of **OsRfPZnOs** demonstrating identity and acceptable purity of the desired compound.

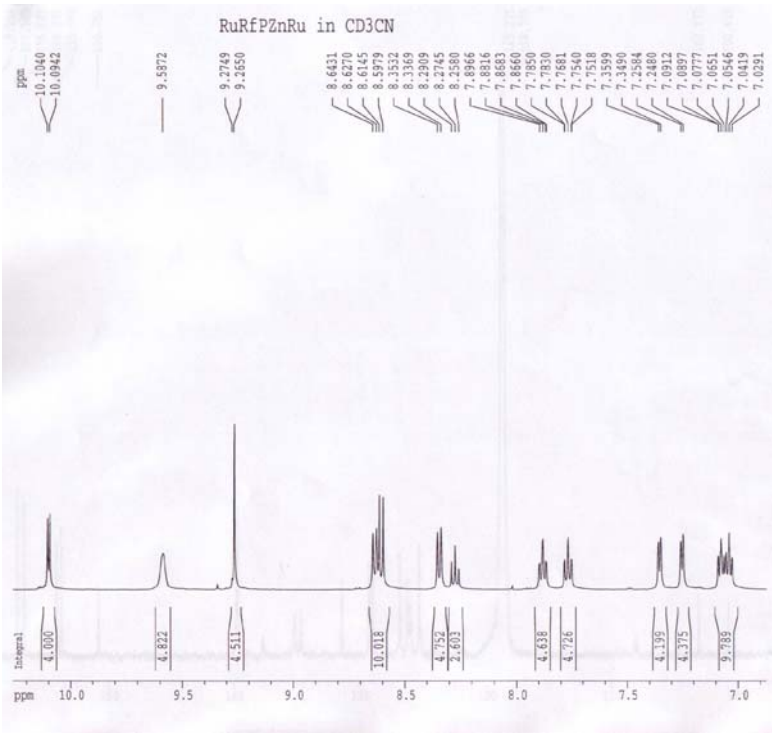

Figure S10A. Aromatic region of the ^{1}H NMR spectrum of **RuRfPZnRu** demonstrating identity and acceptable purity of the desired compound.

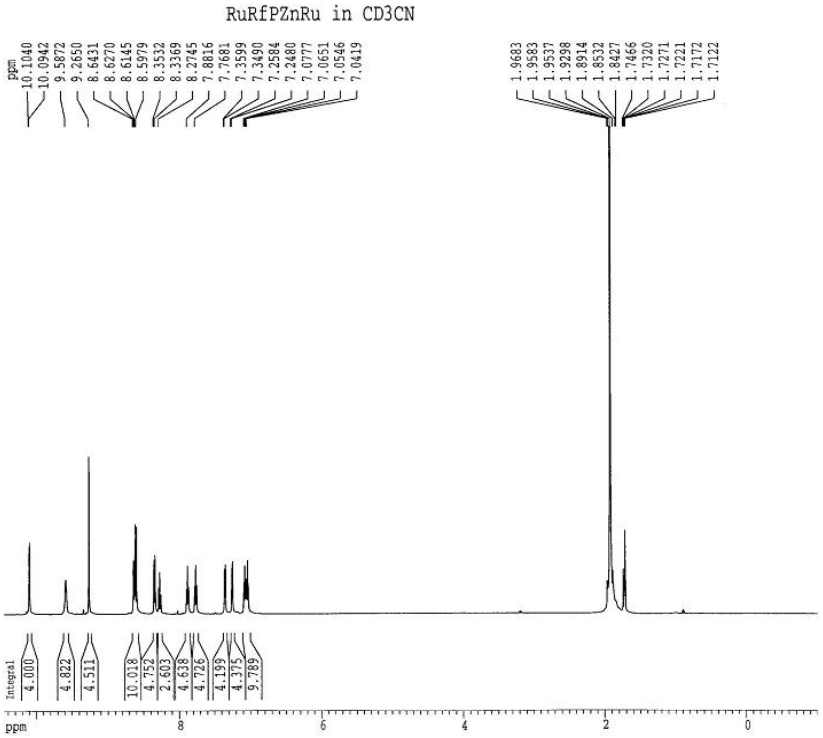

Figure S10B. Full ^{1}H NMR spectrum of **RuRfPZnRu**.

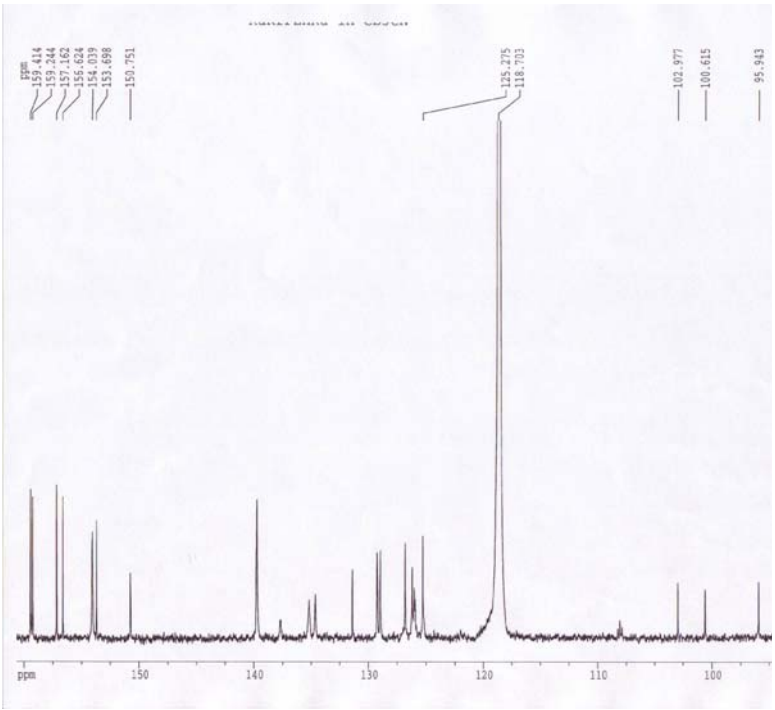

Figure S11A. Aromatic region of the proton-decoupled ^{13}C NMR spectrum of **RuRfPZnRu** demonstrating identity and acceptable purity of the desired compound. Note that the number of observed peaks does not exactly correspond to the number of carbon nuclei in this compound as a result of complications due to ^{13}C-^{19}F spin-spin interactions.

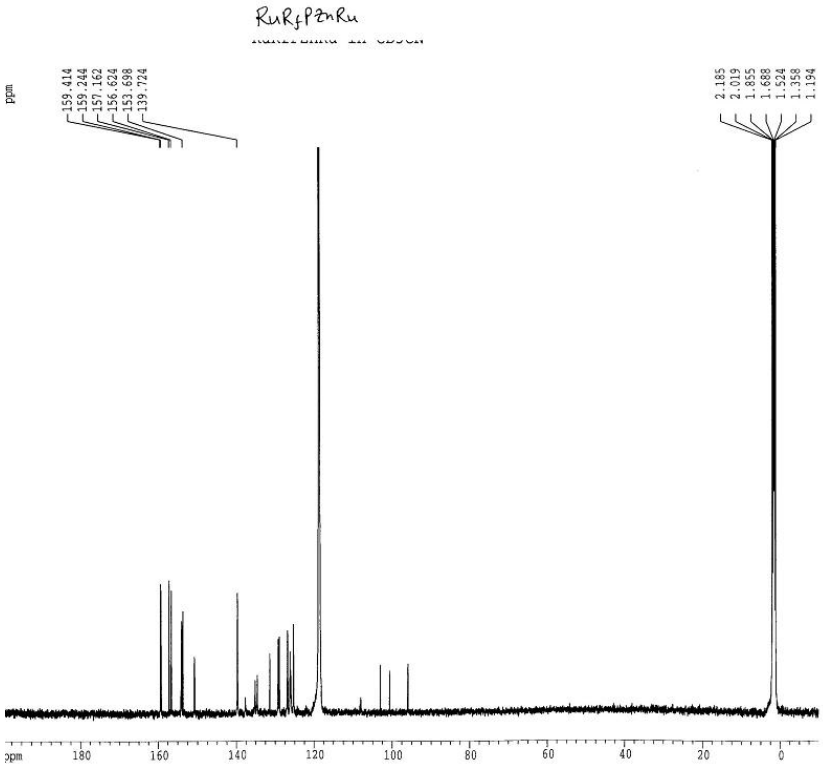

Figure S11B. Full proton-decoupled ^{13}C NMR spectrum of **RuRfPZnRu.**

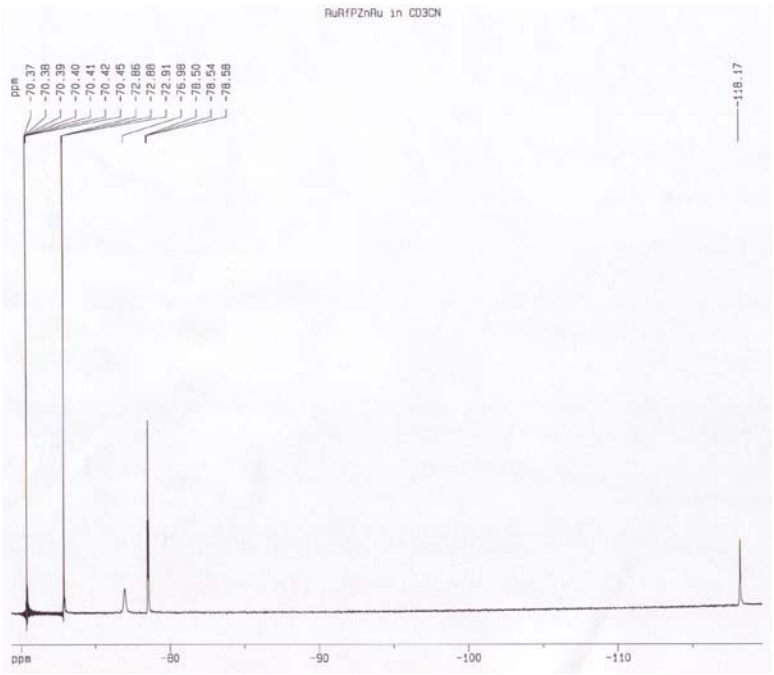

Figure S12. ^{19}F NMR spectrum of **RuRfPZnRu** demonstrating identity and acceptable purity of the desired compound.

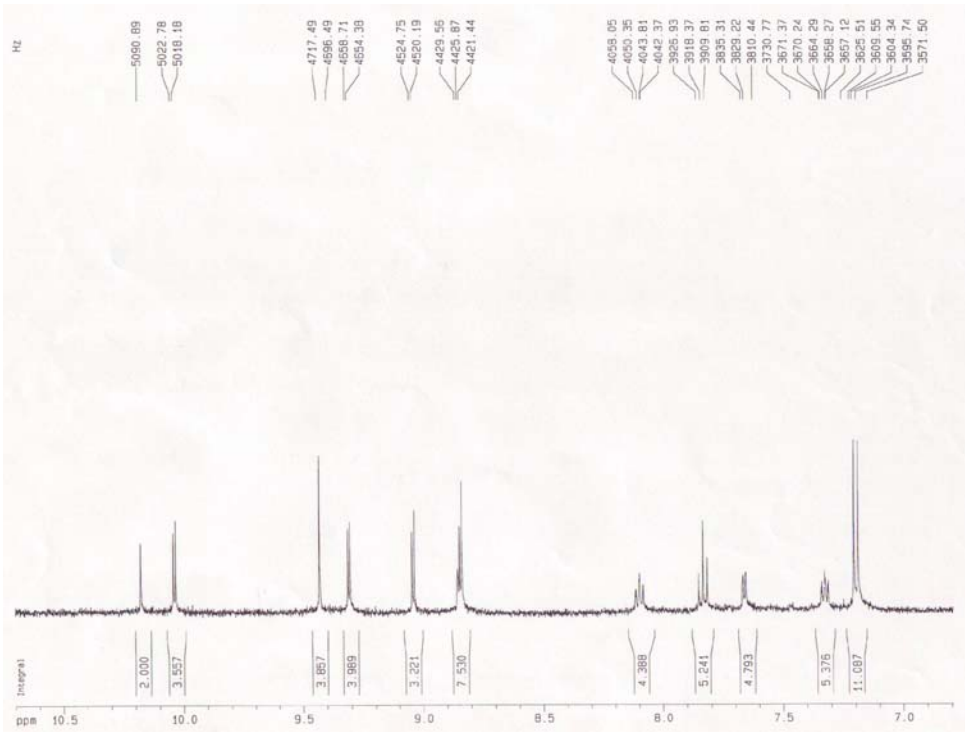

Figure S13A. Aromatic region of the ^{1}H NMR spectrum of **PZnRuPZn** demonstrating identity and acceptable purity of the desired compound.

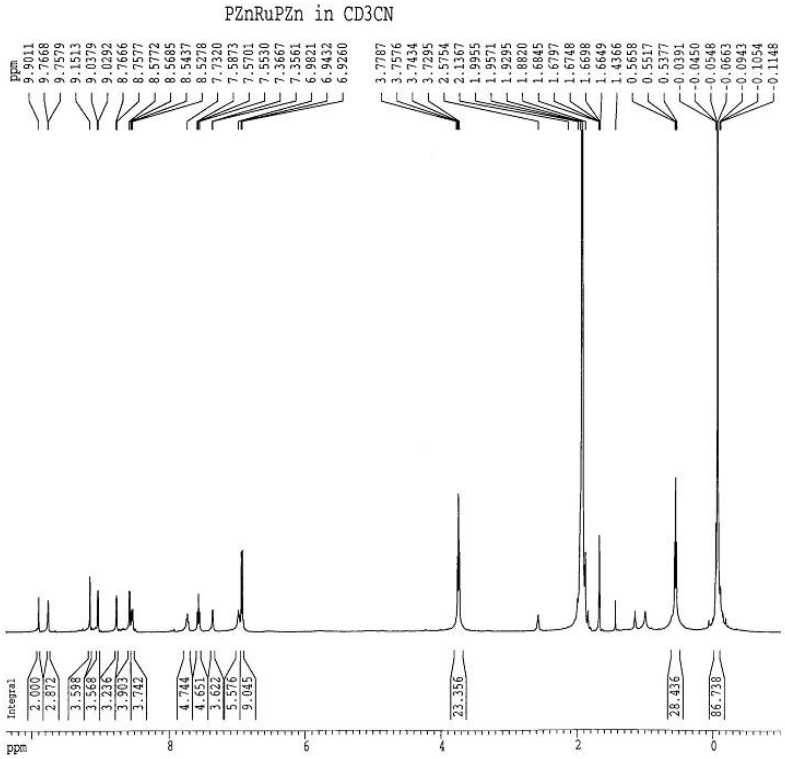

Figure S13B. Full ^{1}H NMR spectrum of **PZnRuPZn.**

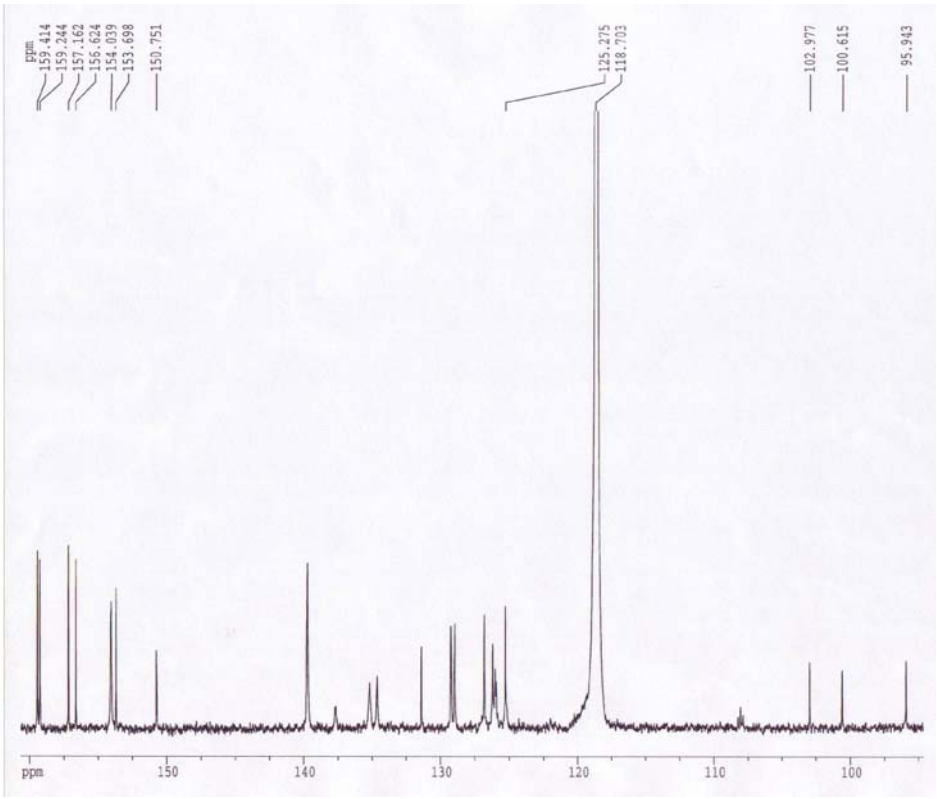

Figure S14A. Aromatic region of the proton-decoupled ^{13}C NMR spectrum of **PZnRuPZn** demonstrating identity and acceptable purity of the desired compound

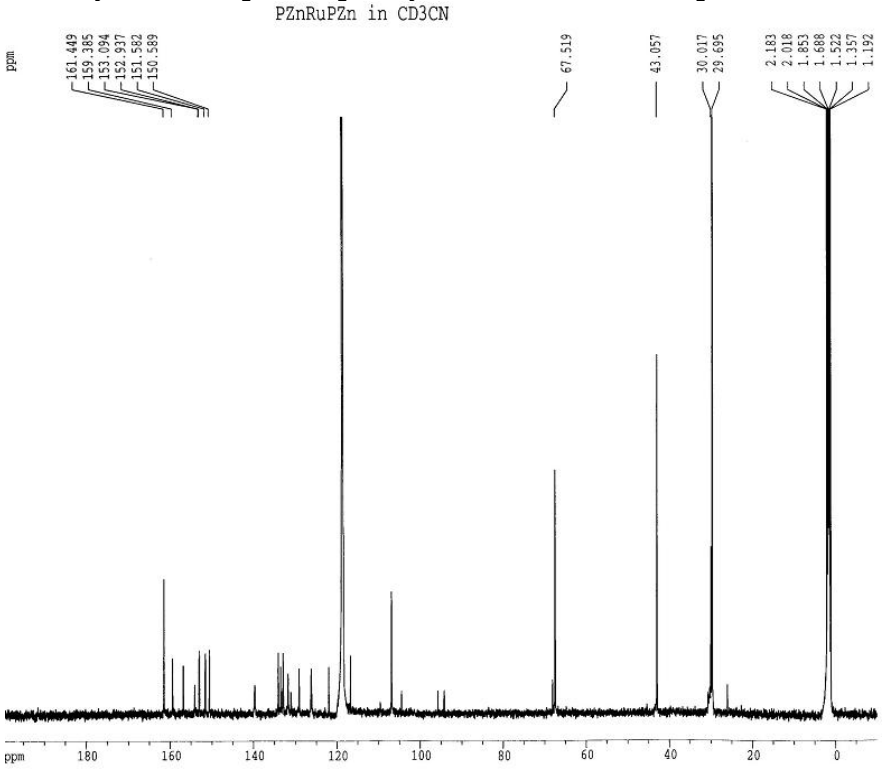

Figure S14B. Full proton-decoupled ^{13}C NMR spectrum of **PZnOsPZn**.

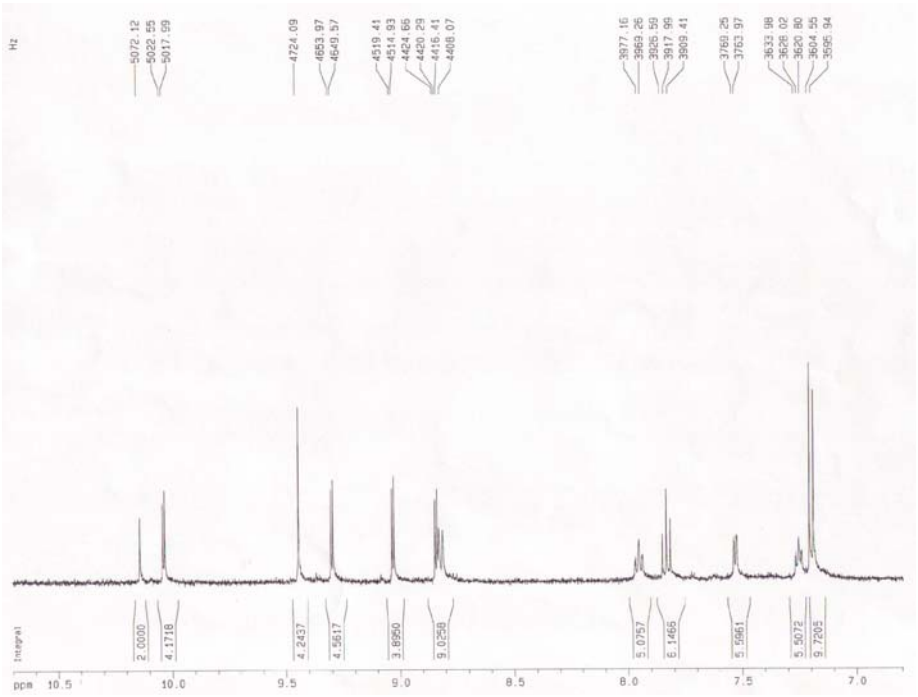

Figure S15A. Aromatic region of the ^{1}H NMR spectrum of **PZnOsPZn** demonstrating identity and acceptable purity of the desired compound.

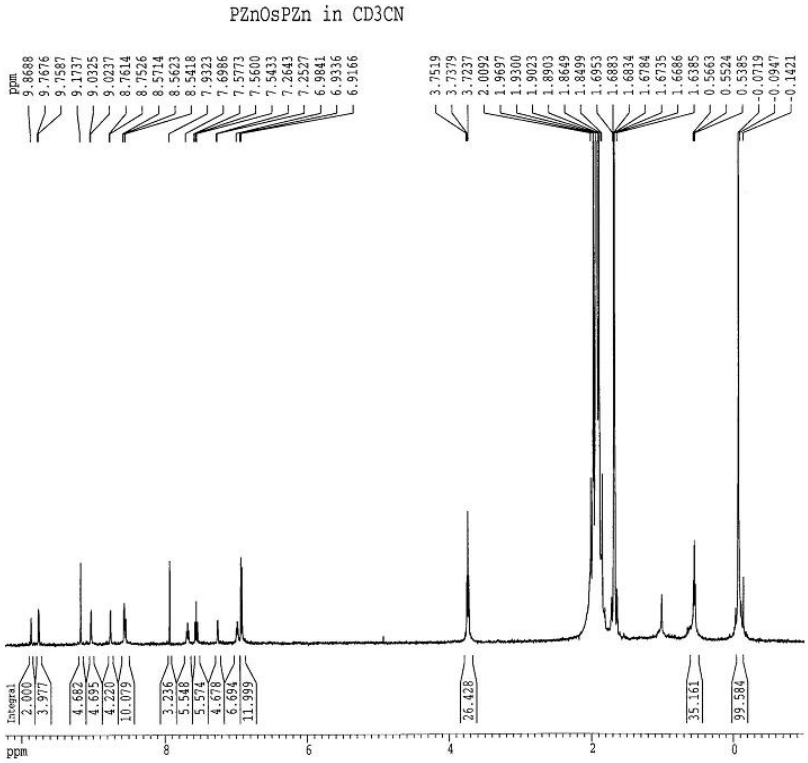

Figure S15B. Full ^{1}H NMR spectrum of **PZnOsPZn**.

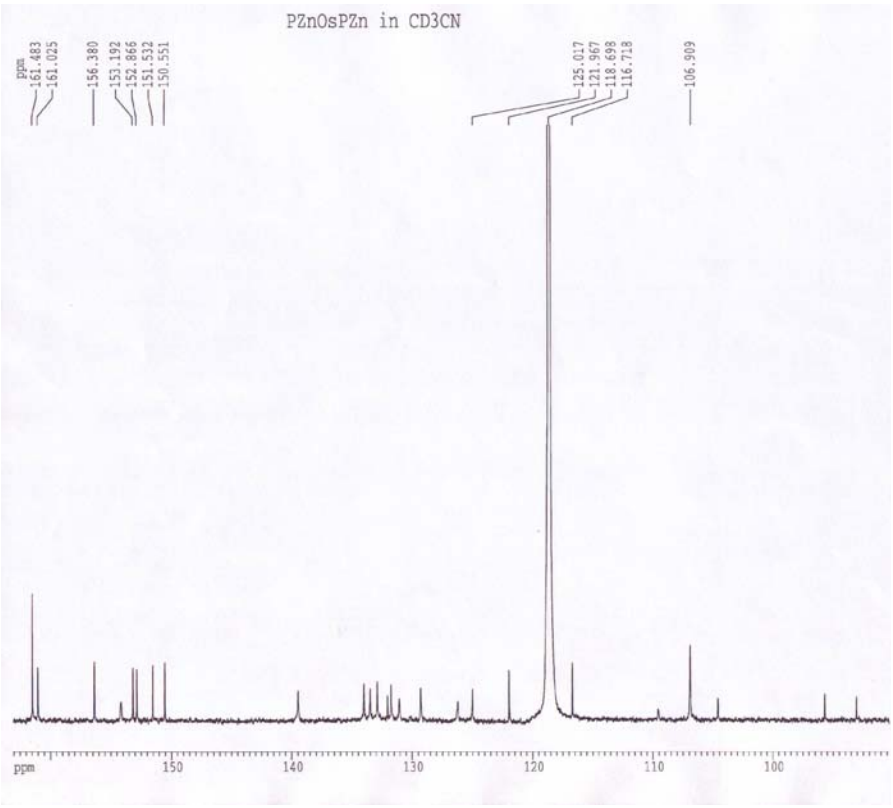

Figure S16A. Aromatic region of the proton-decoupled ^{13}C NMR spectrum of **PZnOsPZn** demonstrating identity and acceptable purity of the desired compound

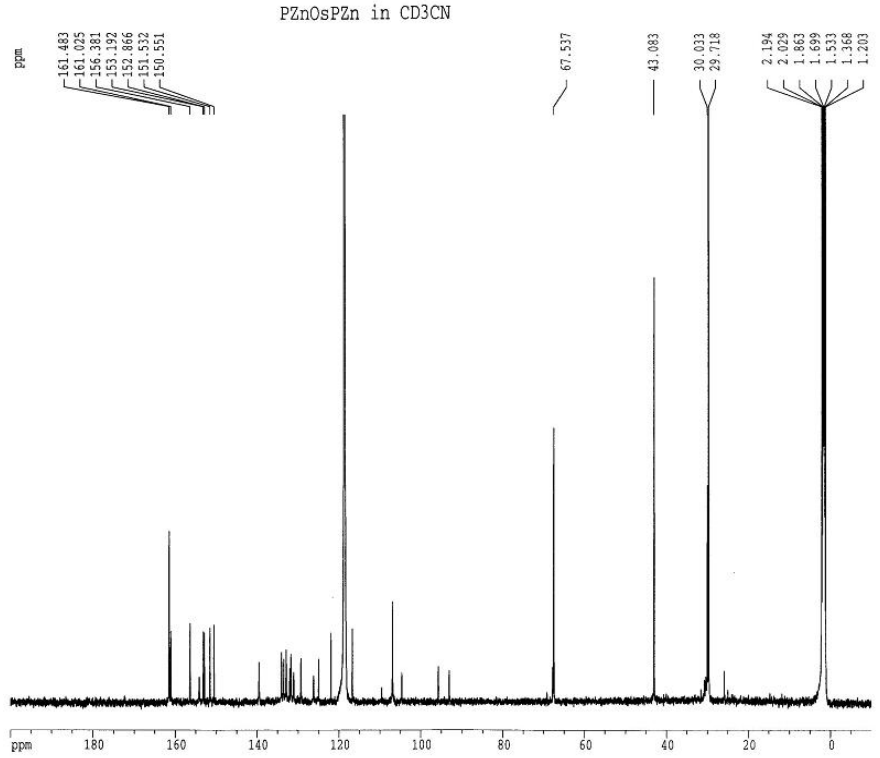

Figure S16B. Full proton-decoupled ^{13}C NMR spectrum of **PZnOsPZn**.

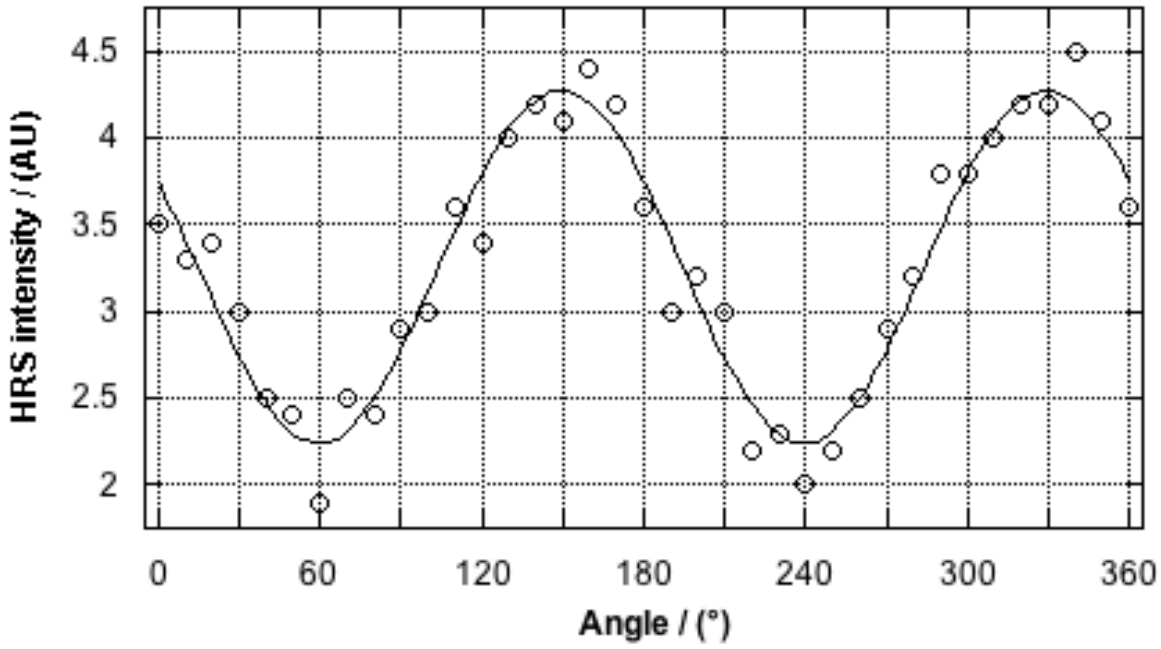

Figure S17. Dependence of measured HRS intensity upon the angle between the polarized incident irradiation pulse and the detector for **OsR$_f$PZnOs**. Experimental conditions: λ_{inc} = 800 nm; T = 20 ºC; solvent = CH_3CN.

References for Supporting Information

[1] H. T. Uyeda, Y. X. Zhao, K. Wostyn, I. Asselberghs, K. Clays, A. Persoons, M. J. Therien, *J. Am. Chem. Soc.* **2002**, *124*, 13806.
[2] T. V. Duncan, I. V. Rubtsov, H. T. Uyeda, M. J. Therien, *J. Am. Chem. Soc.* **2004**, *126*, 9474.
[3] P. R. Frail, T. V. Duncan, H. T. Uyeda, M. J. Therien, *Manuscript in Preparation.*
[4] K. Clays, A. Persoons, *Phys. Rev. Lett.* **1991**, *66*, 2980.
[5] G. Olbrechts, R. Strobbe, K. Clays, A. Persoons, *Rev. Sci. Inst.* **1998**, *69*, 2233.
[6] G. J. T. Heesink, A. G. T. Ruiter, N. F. van Hulst, B. Bolger, *Phys. Rev. Lett.* **1993**, *71*, 999.
[7] T. Verbiest, K. Clays, C. Samyn, J. Wolff, D. Reinhoudt, A. Persoons, *J. Am. Chem. Soc.* **1994**, *116*, 9320.
[8] E. Hendrickx, A. Vinckier, K. Clays, A. Persoons, *J. Phys. Chem.* **1996**, *100*, 19672.
[9] I. D. Morrison, R. G. Denning, W. M. Laidlaw, M. A. Stammers, *Rev. Sci. Inst.* **1996**, *67*, 1445.
[10] C. Boutton, K. Clays, A. Persoons, T. Wada, H. Sasabe, *Chem. Phys. Lett.* **1998**, *286*, 101.
[11] J. Zyss, I. Ledoux, *Chem. Rev.* **1994**, *94*, 77.